Original Paper

Cellular Physiology and Biochemistry

Cell Physiol Biochem 2005;16:119-126

Accepted: November 18, 2004

The Role of Ca^{2+} Transport Across the Plasma Membrane for Cell Migration

Vladyslav Dreval, Peter Dieterich*, Christian Stock and Albrecht Schwab

Institute of Physiology II, Universität Münster, *Physiologisches Institut, Medizinische Fakultät Carl Gustav Carus Dresden

Key Words

Cell migration • Ca^{2+} • Na^+/Ca^{2+} exchange • Plasma membrane Ca^{2+}-ATPase

Abstract

Cell migration plays a central role in many physiological and pathophysiological processes. On a cellular level it is based on a highly coordinated restructuring of the cytoskeleton, a continuous cycle of adhesion and de-adhesion as well as on the activity of ion channels and transporters. The cytoplasmic Ca^{2+} ($[Ca^{2+}]_i$) concentration is an important coordinator of these intracellular processes. Thus, $[Ca^{2+}]_i$ must be tightly controlled in migrating cells. This is among other things achieved by the activity of Ca^{2+} permeable channels, the plasma membrane Ca^{2+}-ATPase (PMCA) and the Na^+/Ca^{2+} exchanger (NCX) in the plasma membrane. Here, we wanted to determine the functional role of these transport proteins in cell migration. We therefore quantified the acute effect of inhibitors of these transport proteins (Gd^{3+}, vanadate, KB-R7943) on migration, $[Ca^{2+}]_i$, and intracellular pH (pH_i) of MDCK-F cells. Migration was monitored with computer-assisted time-lapse video microscopy. $[Ca^{2+}]_i$ and pH_i were measured with the fluorescent indicators fura-2 and BCECF. NCX expression in MDCK-F cells was verified with ion substitution experiments, and expression of PMCA was tested with RT-PCR. All blockers lead to a rapid impairment of cell migration. However, the most prominent effect is elicited by NCX-inhibition with KB-R7943. NCX-blockade leads to an almost complete inhibition of migration which is accompanied by a dose-dependent increase of $[Ca^{2+}]_i$ and an intracellular alkalinisation. We show that inhibition of NCX and PMCA strongly affects lamellipodial dynamics of migrating MDCK-F cells. Taken together, our results show that PMCA and in particular NCX are of critical importance for cell migration.

Introduction

Cell migration plays an important role in many physiological and pathophysiological processes such as embryogenesis, immune defense, wound healing or formation of tumor metastases. Cell migration depends on a complicated interplay of cytoskeletal reorganization [1, 2], formation and release of cell-matrix contacts [3],

KARGER

Fax +41 61 306 12 34
E-Mail karger@karger.ch
www.karger.com

1015-8987/05/0163-0119$22.00/0

Accessible online at:
www.karger.com/journals/net

Albrecht Schwab
Institut of Physiology II
Robert-Koch-Str. 27b, D-48149 Münster (Germany)
Tel. +49 251 8355329, Fax +49 251 8355331
E Mail aschwab@uni-muenster.de

membrane recycling [4] and activity of ion transporters and channels [5]. All these processes are required for optimal cell migration. Several studies showed that the intacellular Ca^{2+} concentration ($[Ca^{2+}]_i$) is an important coordinator of different mechanisms required for cell migration [6]. Elevations of $[Ca^{2+}]_i$ support the detachment of integrins from their extracellular ligands [7], they promote the contraction of the cortical actomyosin network [8], and they also activate Ca^{2+} sensitive K^+ channels [9].

While the importance of $[Ca^{2+}]_i$ as an essential regulator of cell migration is well established, less is known about transport processes across the plasma membrane involved in maintaining the intracellular Ca^{2+} homeostasis of migrating cells and thereby about the role of the respective transport proteins in cell migration. Studies in other non-excitable cell types revealed at least three major transport pathways across the plasma membrane [10]: a Ca^{2+} influx pathway via Ca^{2+} channels (for example mechano-sensitive or store-operated channels), and two Ca^{2+} export pathways (plasma membrane Ca^{2+}-ATPase (PMCA) and Na^+/Ca^{2+} exchanger (NCX)). The Ca^{2+} influx pathway can be blocked with Gd^{3+} [11]. Inhibitors for PMCA and NCX are vanadate (V^{5+}) [12] and KB-R7943 [13], respectively. We used these inhibitors as tools to investigate the functional roles of the Ca^{2+} influx pathway and of PMCA and NCX for cell migration. We determined the effects of these inhibitors on migration, the intracellular Ca^{2+} concentration, and the intracellular pH of transformed renal epithelial cells (MDCK-F cells). Our results show that the lamellipodium of MDCK-F cells appears to be the main target of these inhibitors and that NCX activity is of particular importance for cell migration.

Materials and Methods

Chemicals

All chemicals were purchased from Sigma (Deisenhofen, Germany) unless stated differently. The inhibitor of the Na^+/Ca^{2+} exchanger, KB-R7943, was a kind gift from Koichi Yokota (Nippon Organon, K.K., Osaka, Japan). KB-R7943 was dissolved in DMSO (stock solution 250 mmol/l) and used in concentrations of 100 nmol/l - 100 µmol/l. Gd^{3+} (inhibitor of Ca^{2+} permeable channels; [11]) and V^{5+} (inhibitor of the plasma membrane Ca^{2+}-ATPase; [14]) were used in concentrations of 50 µmol/l and 10 - 150 µmol/l, respectively.

Cell culture

Experiments were carried out on transformed Madin-Darby canine kidney (MDCK-F) cells [15] grown in bicarbonate-buffered Minimal Essential Medium (MEM; pH 7.4) with Earle's salts (Biochrom, Berlin, Germany) supplemented with 10% fetal calf serum (Biochrom). Cells were kept at 37°C in humidified air containing 5% CO_2. MDCK-F cells were seeded at low density on poly-L-lysin coated glass cover slips 1 to 2 days prior to migration experiments or measurements of the intracellular Ca^{2+} concentration.

Migration experiments

Migration of MDCK-F cells was captured by means of high resolution time lapse video microscopy. Glass cover slips with the cells were placed in a heating chamber (37°C) on the stage of a phase contrast microscope (ID03, 32x; Zeiss, Oberkochen, Germany) and superfused with prewarmed Ringer´s solution containing (in mmol/l): NaCl 122.5, KCl 5.4, $CaCl_2$ 1.2, $MgCl_2$ 0.8, NaH_2PO_4 0.1, glucose 5.5, HEPES 10, pH 7.4. NaH_2PO_4 was omitted when Gd^{3+} was used. The protocol of all migration experiments was such that a 10 min control period was followed by a 10 min experimental period during which the Ringer´s solution was supplemented with various inhibitors. Migration was monitored with a video camera (Hamamatsu, Hersching, Germany) controlled by HiPic software (Hamamatsu). Images were taken in 10 s intervals and stored as stacks of Tiff-files.

Data analysis of migration experiments

A) Image segmentation. Image segmentation was performed with Amira software (TGS). Image stacks of the experiments were loaded into Amira (TGS, France; http://www.amiravis.com/). The outlines of individual cells or of their lamellipodium and cell body were marked semiautomatically at each time step throughout the entire image stack. The lamellipodium was defined as the part of the cell in which no organellar or vesicular structures were visible in phase contrast images. Usually, a sharp transition from the cell body to the lamellipodium could be detected. These segmentation data were used for further processing [16].

B) Data handling. Customized JAVA classes and programs (http://java.sun.com/) were developed to manage information on the experimental setup (microscope magnification, time interval). ImageJ classes (http://rsb.info.nih.gov/ij/) allowed handling of the original and segmented image data. Quantitative data analysis and calculation of parameters were performed with JAVA programs developed by ourselves.

C) Calculation of area and velocity of migrating cells. Time-dependent cell outlines derived from image segmentations were the basis of all further calculations. The x- and y-coordinates of the cell center (µm) were determined as geometric mean of equally weighted pixel positions within the cell outlines. Hence, the time sequence of the cell center (x(t), y(t)) represents the trajectory of the moving cell during the course of an experiment. The velocity of migrating cells (v(t); µm/min) was calculated for 10 s intervals from trajectories as the movement of the cell center by applying a three point difference quotient. Cell areas (A; μm^2) are defined as the appropriately scaled sum of all pixels inside the cell´s contours.

Determination of the cytosolic free Ca^{2+} concentration

We determined the free cytosolic Ca^{2+} concentration ($[Ca^{2+}]_i$) employing the fluorescent Ca^{2+} indicator fura-2 ([17]; Molecular Probes, Eugene, OR, USA) by using video imaging techniques as described previously [18]. For dye-loading MDCK-F cells were incubated in culture medium containing 5 µmol/l fura-2 AM for 30 - 45 min in the dark at 37°C. Coverslips were placed on the stage of an inverted microscope (x100 oil immersion objective; Axiovert TV 100, Zeiss, Oberkochen, Germany) and continuously superfused with prewarmed (37°C) Ringer solution. By changing the appropriate filters the excitation wavelength alternated between 334 and 380 nm, respectively. The emitted fluorescence was monitored at 500 nm with an ICCD camera (Atto Instruments, Rockville, MD, U.S.A.). Filter change and data acquisition were controlled by Attofluor software (Atto Instruments). Up to 20 regions of interest, each corresponding to approximately 150 pixels, were placed over cell body and lamellipodium of individual MDCK-F cells. Average fluorescence intensities in these areas were measured in 10 s intervals.

$[Ca^{2+}]_i$ was calculated according to the equation $[Ca^{2+}]_i = K_d \times ß \times (R - R_{min})/ (R_{max} - R)$ [17]. K_d is the dissociation constant of 225 nmol/l, R_{min} and R_{max} are fluorescence ratios at zero and saturating Ca^{2+} after excitation with 334 and 380 nm, respectively. ß is a factor obtained by dividing fluorescence intensity after excitation with 380 nm obtained at zero Ca^{2+} by the 380 nm value measured at saturating Ca^{2+}. Ca^{2+} measurements were calibrated at the end of each experiment. R_{max}, R_{min} and ß were determined by the application of ionomycin-containing (2 µmol/l) Ringer solutions containing either 5 mmol/l Ca^{2+} or 5 mmol/l EGTA. R_{max}, R_{min} and ß were determined separately for each region. The experimental protocol of measurements of $[Ca^{2+}]_i$ was the same as that of migration experiments: a 10 min control period was followed by a 10 min experimental period during which inhibitors were applied.

Determination of pH_i

pH_i of MDCK-F cells was measured by using video imaging techniques and the fluorescent pH indicator BCECF (Molecular Probes, Eugene, OR, USA). For dye-loading MDCK-F cells were incubated in culture medium containing 2 µmol/l BCECF-AM for 1 to 2 min. Coverslips were placed on the stage of an inverted microscope (Axiovert TV 100, Zeiss, Oberkochen, Germany) and continuously superfused with prewarmed (37°C) Ringer's solution. Excitation wavelength alternated between 488 nm and 460 nm, respectively. The emitted fluorescence was monitored at 500 nm with an ICCD camera (Atto Instruments, Rockville, MD, USA). Filter change and data acquisition were controlled by Attofluor software (Atto Instruments). Average fluorescence intensities (corrected for background fluorescence) were measured at 20 s intervals in several demarcated regions of interest placed over the projected cell surface.

At the end of each experiment pH_i measurements were calibrated by superfusing MDCK-F cells with a modified Ringer solution (in mmol/l: 125 KCl, 1 $MgCl_2$, 1 $CaCl_2$, 20 HEPES) containing 10 µmol/l nigericin using a 2-point calibration (pH 7.5 and pH 6.5).

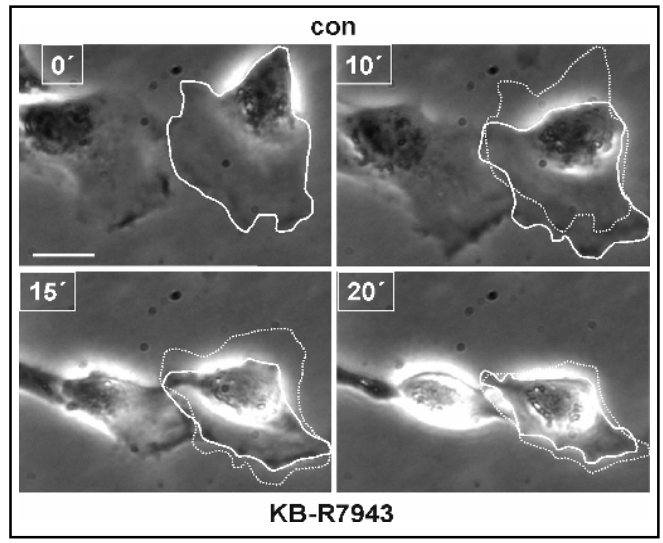

Fig. 1. Migrating MDCK-F cells. The cell labelled with a solid line is shown at the beginning of the experiment (0´) and 10´, 15´ and 20´ later. The dotted line shows the position of the same cell in the preceeding panels. The upper two panels show the behavior of MDCK-F cells under control conditions, the lower two panels in the presence of the NCX-blocker KB-R7943 (100 µmol/l). Bar: 20 µm.

RT-PCR experiments

Total RNA from MDCK-F cells grown to subconfluency was isolated with RNeasy spin columns (Qiagen, Hilden, Germany) 1 day after plating. 2 µg of RNA were used for cDNA synthesis with Superscript III reverse transcriptase (Gibco BRL) using oligo$(dT)_{16}$ primers. We used the following primers (20) for amplifying fragments of PMCA1 and PMCA4 from MDCK-F cells with a Progene thermocycler: 5´-CAATGGCTGTGGTCCATATTC-3´, 5´-GTCATCTTCAGCATCAGTGTC-3´; 5´-TGGTCTTCACGCTCTTGTTCG-3´, 5´-GCCAGGTCATCTCTGCAATAC-3´, 5´-ATCCGCGACTTAGAAGCCAAC-3´. The annealing temperature was 53°C. Amplified cDNA fragments were size-fractionated in a 6 % polyacrylamide gel and stained with SYBR Gold (Molecular Probes, Portland, OR, USA).

Statistics

Data are presented as means ± SEM. In figs. 4 and 5 we present weighted mean values that were calculated according to $\langle x_i \rangle = (x_{i-2} + 2x_{i-1} + 4x_i + 2x_{i+1} + x_{i+2})/10$. Statistical significance was tested with paired or unpaired Student´s t-test where applicable. Significance was assumed when $p < 0.05$.

Results

Migration experiments

MDCK-F cells migrate under control conditions at a rate of 1.84 ± 0.05 µm/min (n = 119). It is conspicuous

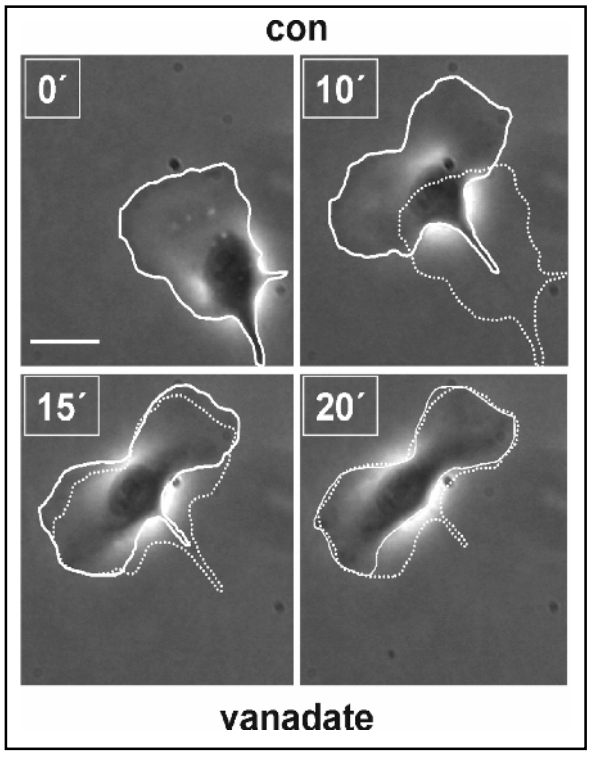

Fig. 2. Migrating MDCK-F cell. The outlines of the cell are labelled with a solid line at the beginning of the experiment (0´) and 10´, 15´ and 20´ later. The dotted line shows the position of the cell in the preceeding panels. The upper two panels show the behavior under control conditions, the lower two panels in the presence of the PMCA-blocker vanadate (150 µmol/l). Bar: 20 µm.

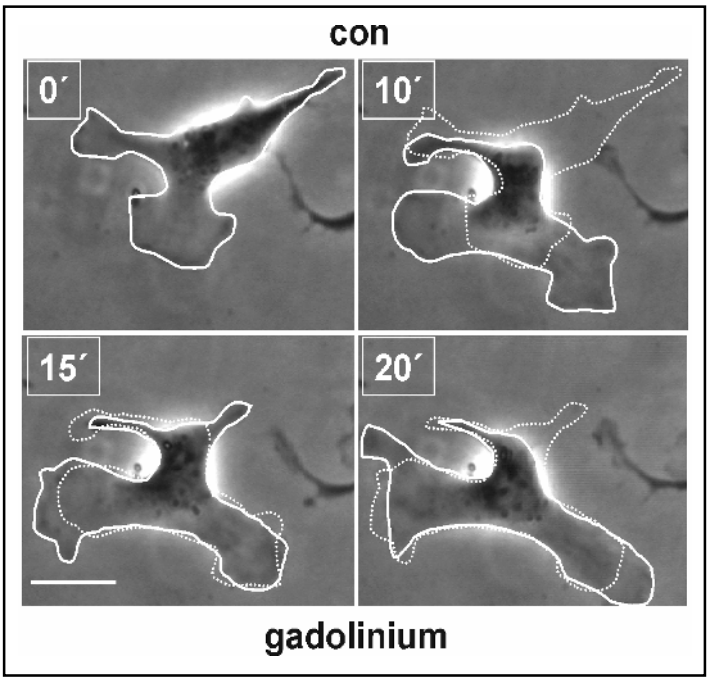

Fig. 3. Migrating MDCK-F cell. The outlines of the cell are labelled with a solid line at the beginning of the experiment (0´) and 10´, 15´ and 20´ later. The dotted line shows the position of the cell in the preceeding panels. The upper two panels show the behavior under control conditions, the lower two panels in the presence of gadolinium (50 µmol/l). Bar: 20 µm.

that this value is twice as high as that reported previously [9]. This difference is due to the high time resolution of our present migration experiments in which images were captured at 10 s intervals while we used 1 - 5 min intervals in our previous studies. When we calculate the rate of migration for a sampling interval of 1 min we obtain values similar to those reported earlier (1.25 ± 0.06 µm/min; n = 20; [19]). The higher rate of migration with a 10 s sampling interval is largely due to the fast remodeling at the leading edge of the lamellipodium which results in an apparent "zigzag"-movement of the cell center. Thus, the analysed crawling path becomes longer when migration is monitored with high time resolution. The contribution of this "biological noise" to the calculated rate of migration becomes smaller when the time interval is increased. Then the contribution of the cell´s translocation on the calculated position of the cell center predominates.

Migratory activity is inhibited when the intracellular Ca^{2+} homeostasis is perturbed by blocking Ca^{2+} extrusion via the Na^{+}/Ca^{2+} exchanger with KB-R7943 (100 µmol/l; n = 9; see figs. 1 and 4A). MDCK-F cells come to a complete stop within 10 min. Lamellipodia are withdrawn and the cell body is retracted (fig. 1). These pronounced morphological changes, however, shift the center of gravity, so that the calculated rate of migration (1.12 ± 0.09 µm/min after 10 min KB-R7943) overestimates the "true" migratory activity. Instead, the best way to quantify the effect of KB-R7943 on migration of MDCK-F cells is the determination of their projected cell area. It decreases after a lag period of approximately 1.5 min from 1305 ± 108 μm^2 to reach a value of 415 ± 42 μm^2 after 10 min (see fig. 4A).

A similar response is observed when MDCK-F cells are exposed to V^{5+} (n = 14; 150 µmol/l; see figs. 2 and 4B). However, the inhibition of migration and morphological changes are not as pronounced and rapid as those caused by KB-R7943. The cell area is reduced from 1300 ± 71 μm^2 to 983 ± 72 μm^2 (see fig. 4B). This is accompanied by a fall of the rate of migration from 1.84 ± 0.06 µm/min to 1.03 ± 0.14 µm/min after 10 min. The inhibition is dose-dependent, the half-maximal inhibitory concentration being approximately 15 µmol/l (see inlet in fig. 4B).

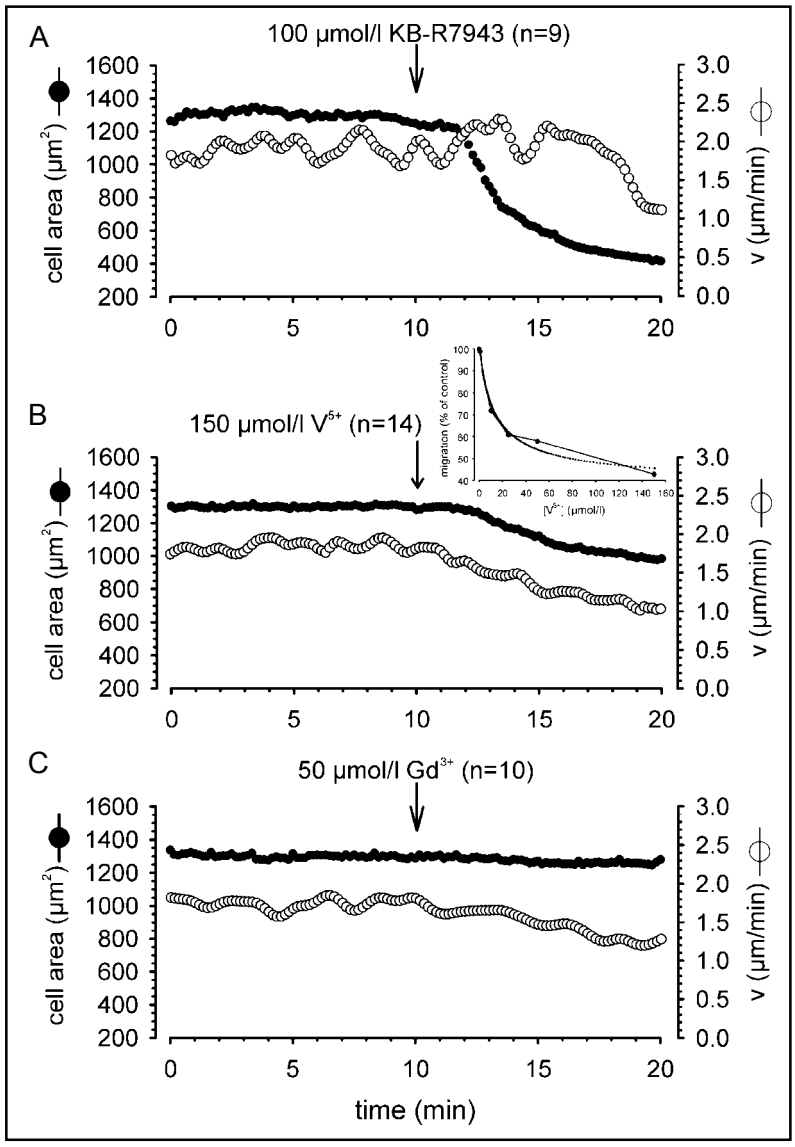

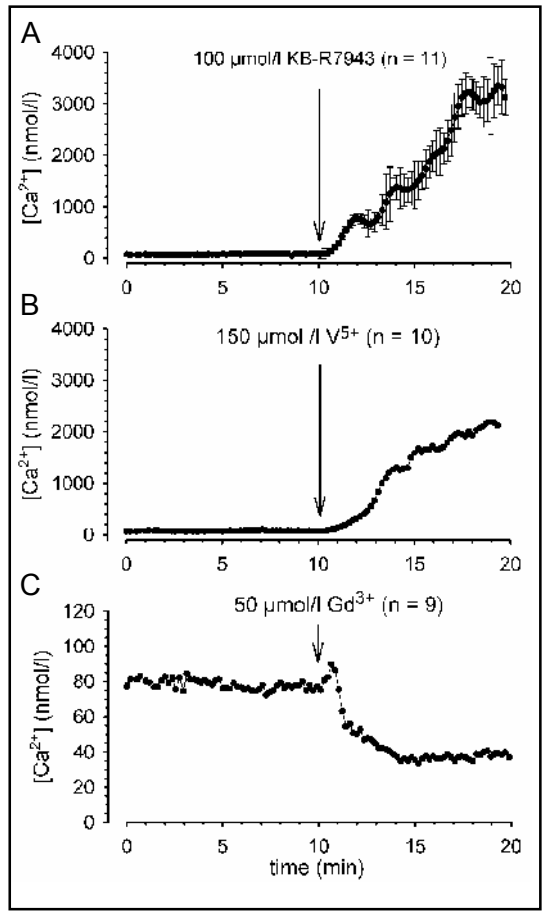

Fig. 5. Summary of measuremnts of the cytoplasmic Ca^{2+} concentration ($[Ca^{2+}]_i$). Data are calculated in 10 s intervals and averaged for the indicated number of cells. A: Effect of the NCX inhibitor KB-R7943 (100 µmol/l). B: Effect of PMCA inhibitor V^{5+} (150 µmol/l). C: Effect of blocking Ca^{2+} influx with Gd^{3+}.

△

Fig. 4. Summary of migration experiments. The closed symbols represent the projected cell area (in μm^2) and the open symbols the rate of migration (in µm/min) of MDCK-F cells. Data are calculated in 10 s intervals. A: Effect of the NCX inhibitor KB-R7943 (100 µmol/l). B: Effect of PMCA inhibitor V^{5+} (150 µmol/l). The inlet shows a dose-response curve in which the rate of migration (normalized to the respective control values) is plotted as a function of the V^{5+} concentration. C: Effect of blocking Ca^{2+} influx with Gd^{3+}.

Blocking Ca^{2+} influx with Gd^{3+} (50 µmol/l; n = 10) has a rather moderate effect on migration of MDCK-F cells. The cell area is virtually unchanged (1287 ± 118µm² under control conditions versus 1247 ± 129 µm² in the presence of Gd^{3+}, see figs. 3 and 4C). The rate of migration decreases from 1.75 ± 0.11 µm/min to 1.31 ± 0.04 µm/min ($p < 0.05$). Collectively, these data indicate that the application of KB-R7943 (inhibition of the Na^+/Ca^{2+} exchanger) has the strongest short term effect on migration of MDCK-F cells.

Intracellular Ca^{2+} concentration

We quantified the effect of the aforementioned inhibitors in separate measurements of $[Ca^{2+}]_i$. KB-R-7943 (100 µmol/l; n = 11; see fig. 5A) elicits an immediate and sustained rise of $[Ca^{2+}]_i$ to 3.5 ± 0.05 µmol/l. Fig. 6A shows that this effect is dose-dependent. Already 1 µmol/l KB-R7943 induces a significant rise of $[Ca^{2+}]_i$. The response to V^{5+} (150 µmol/l; n = 10; see fig. 5B) is qualitatively similar, but the onset of the rise of $[Ca^{2+}]_i$ is somewhat delayed, and $[Ca^{2+}]_i$ reaches 2.2 ± 0.05 µmol/

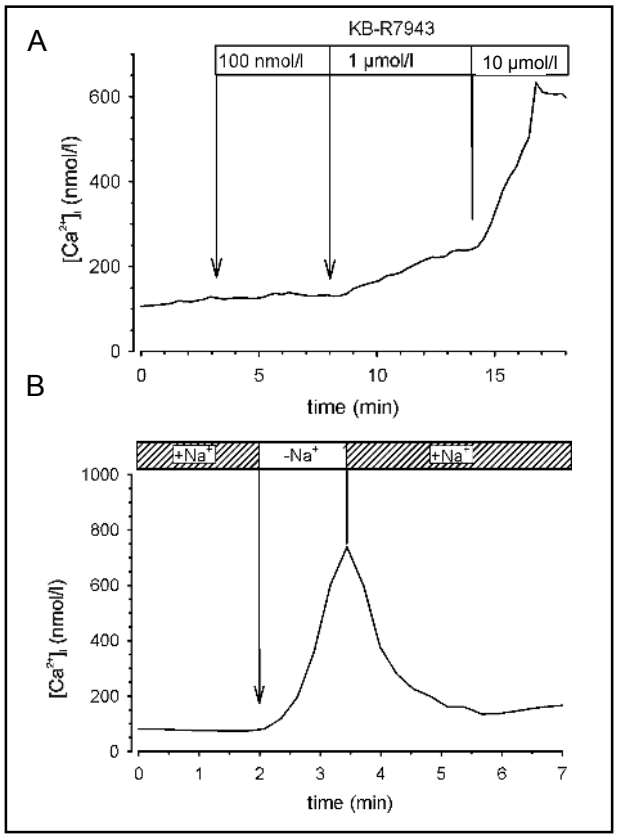

Fig. 6. A) Tracing of an original experiment which shows the dose-dependence of KB-R7943 on $[Ca^{2+}]_i$.1 µmol/l KB-R7943 leads to a significant increase of $[Ca^{2+}]_i$ while 100 nmol/l have almost no effect. The half-maximal effect is achieved with approximately 10 µmol/l. B) Tracing of an original experiment showing NCX activity in MDCK-F cells. Removal of extracellular Na^+ (substituted by $NMDG^+$) leads to a rapid increase of $[Ca^{2+}]_i$ which is reversed by the readdition of Na^+.

l. These data indicate that the Na^+/Ca^{2+} exchanger plays a more important role in Ca^{2+} extrusion in MDCK-F cells than the PMCA. Blocking Ca^{2+} influx with Gd^{3+} (50 µmol/l; n = 9; see fig. 5C) induces a decrease of $[Ca^{2+}]_i$ to 40 ± 2 nmol/l. Gd^{3+} also blunts the KB-R7943- and V^{5+}-induced increase of $[Ca^{2+}]_i$ (data not shown).

NCX activity in MDCK-F cells was shown more specifically with ion-substitution experiments depicted in fig. 6B. Removal of extracellular Na^+ causes a rapid and reversible increase of $[Ca^{2+}]_i$ which is a strong indication of NCX activity in MDCK-F cells. We performed RT-PCR experiments in order to determine the PMCA isoform expressed in MDCK-F cells. Fig. 7 shows that migrating MDCK-F cells express like polarized epithelial MDCK cells the splice variant PMCA1b. However, we did not detect PMCA4.

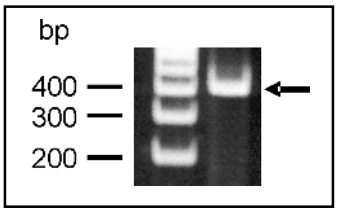

Fig. 7. RT-PCR experiments show that migrating MDCK-F cells express the splice variant PMCA1b. The left lane contains the DNA standard, and the right lane shows the PMCA1b amplimer (expected size: 393 bp) (arrow). The respective RT^- controls produced no amplimers.

In fig.8A we plotted the projected cell area of migrating MDCK-F cells as a function of their cytoplasmic Ca^{2+} concentration in the presence of KB-R7943, V^{5+}, and Gd^{3+}. Data points from migration experiments were matched as to time with data points from Ca^{2+} measurements. We calculated the respective mean values for 1 min intervals. It becomes apparent that the cell area which correlates in our study with cell migration strongly depends on the cytoplasmic Ca^{2+} concentration. One can recognize two phases. There is an initial phase during which the cell area only decreases gradually. The onset of this phase occurs when $[Ca^{2+}]_i$ rises above approximately 300 nmol/l and is similar for cells treated with KB-R7943 or V^{5+}. The second phase represents a steep decrease of the projected cell area and occurs in KB-R7943 treated cells when $[Ca^{2+}]_i$ exceeds 600 nmol/l while the projected area of V^{5+}-treated cells only falls when $[Ca^{2+}]_i$ rises above 1 µmol/l. In fig.8B we investigated the reason for this effect. We plotted the areas of lamellipodium and cell body separately. The area of the lamellipodium is strongly dependent on $[Ca^{2+}]_i$ while the cytoplasmic Ca^{2+} concentration has only a minor effect on the area of the cell body of MDCK-F cells. Hence, the decrease of the cell area after inhibition of Na^+/Ca^{2+} exchange or PMCA is largely due to the withdrawal of the lamellipodium of MDCK-F cells.

Intracellular pH

It is remarkable that NCX blockade with KB-R7943 affects the projected cell area at a lower intracellular Ca^{2+} concentration than V^{5+}. Possibly, this difference reflects the influence of NCX on the intracellular Na^+ homeostasis and thereby on other Na^+-transporters like the acid extruding Na^+/H^+ exchanger. We therefore tested whether NCX-blockade also modifies pH_i. The summary of these experiments is shown in fig. 9. pH_i begins to rise after the application of KB-R7943 with a similar time course as $[Ca^{2+}]_i$.

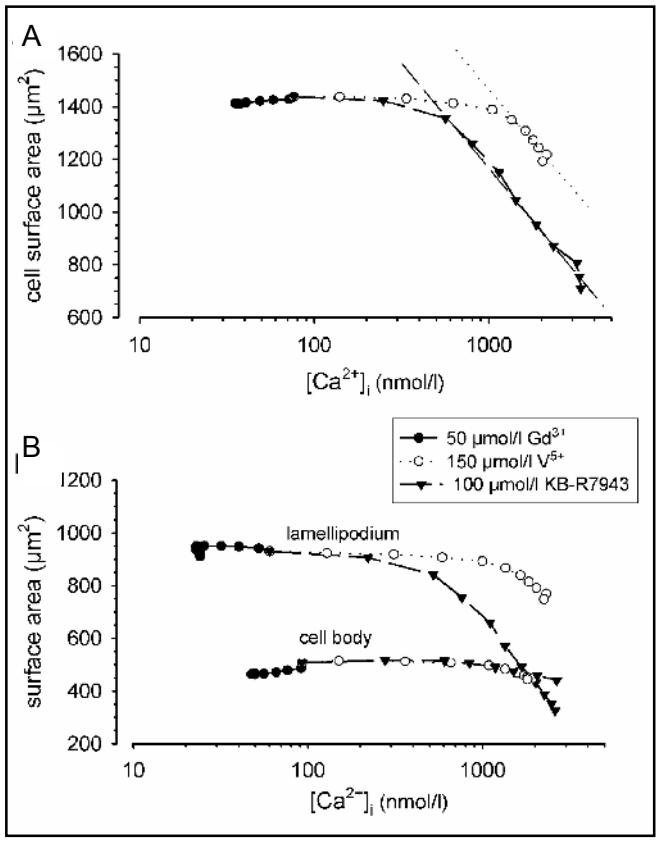

Fig. 8. We plotted the cell area of migrating MDCK-F cells (A) and the areas of lamellipodium and cell body (B) as a function of their cytoplasmic Ca^{2+} concentration measured in the presence of the inhibitors. Areas and $[Ca^{2+}]_i$ values are derived fom the experiments shown in figs. 4 and 5. They are presented as means of 1 min intervals which are matched as to time. Gd^{3+} (l), V^{5+} (o), and KB-R7943(▾).

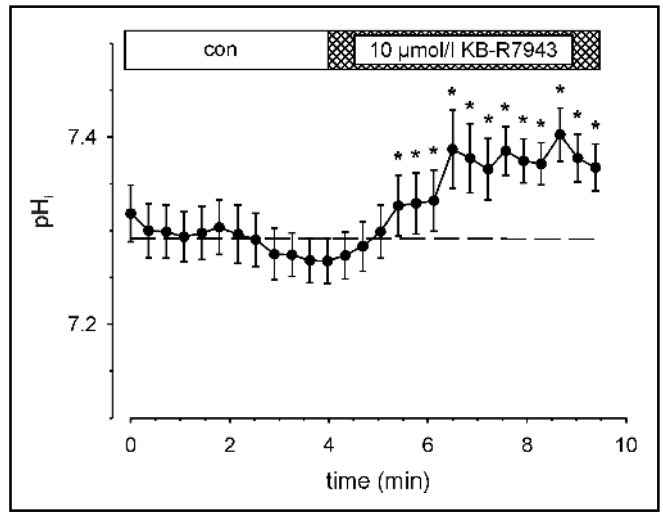

Fig. 9. Summary of pH_i measurements. 10 µmol/l KB-R7943 lead to an intracellular alkalinization. (n = 17). * denotes statistically different from the mean control pH indicated by the dashed line.

Discussion

We could show in our study that three major transport pathways for Ca^{2+} ions across the plasma membrane are required for the normal migratory behavior of MDCK-F cells. Their blockade results in a more or less profound inhibition of migration. The weakest effect is elicited by blocking Ca^{2+} permeable channels with Gd^{3+}, while the NCX inhibitor KB-R7943 has the strongest effect. This is consistent with findings made in epithelial MDCK cells in which NCX is the most important transport protein for transepithelial Ca^{2+} transport [20]. The determination of the cytoplasmic Ca^{2+} concentration revealed that both a decrease of $[Ca^{2+}]_i$ as well as an increase of $[Ca^{2+}]_i$ are accompanied by a reduced rate of migration. A similar behavior was also observed in other cell types. Buffering the cytoplasmic Ca^{2+} in human neutrophils reduces their rate of migration [6], and increasing cytoplasmic Ca^{2+} of glioma cells also leads to an impairment of migration [21]. Thus, the resting Ca^{2+} concentration appears to be the optimal one for migration of MDCK-F cells.

However, it is noteworthy that increasing the cytoplasmic Ca^{2+} concentration does not result in a uniform response with respect to migration of MDCK-F cells. Blockade of the Na^+/Ca^{2+} exchanger inhibits migration at a lower Ca^{2+} concentration than blockade of the Ca^{2+}-ATPase. Our data provide no direct explanation for this phenomenon. However, possibly this discrepancy is related to the different transport properties of NCX and PMCA. It is likely that the blockade of NCX also affects the intracellular Na^+ concentration and thereby modifies the driving force for other Na^+-dependent transporters such as the Na^+/H^+ exchanger. Such a sequence of events could account for the intracellular alkalinisation caused by the inhibition of NCX. Possibly, the combined elevation of $[Ca^{2+}]_i$ and pH_i amplifies the effect of Ca^{2+} ions on the cytoskeletal "migration machinery". Alternatively, inhibition of NCX might result in localized elevations of $[Ca^{2+}]_i$. Such local elevations of $[Ca^{2+}]_i$ that are important for cell migration were shown in neutrophil granulocytes [22]. To our knowledge, the subcellular distribution of NCX and PMCA in migrating cells is not yet known. But it was shown that NCX is concentrated in growth cones of developing neurites - a structure resembling the lamellipodium of migrating cells [23]. Conversely, the PMCA which is part of caveoli [24] may be restricted to

the rear of migrating cells [25]. Such a distinct subcellular distribution could contribute to the generation of local elevations of $[Ca^{2+}]_i$ in the lamellipodium of MDCK-F cells. Finally, we cannot dismiss the possibility that unspecific side effects that are elicited by KB-R7943 or V^{5+} also underly the difference in the apparent Ca^{2+} sensitivity.

Nonetheless, KB-R7943 and V^{5+} appear to affect the same cellular mechanism. The rate at which the cell area or the area of the lamellipodium decrease is identical for both inhibitors. This observation indicates that the lamellipodium of MDCK-F cells is the main effector of the elevated cytoplasmic Ca^{2+} concentration. Dense actin filament networks are the major structural components of lamellipodia and required for cell locomotion. The observation that lamellipodia are retracted following inhibition of NCX or PMCA is, therefore, consistent with the notion that the KB-R7943- and V^{5+}-induced rise of $[Ca^{2+}]_i$ caused a massive depolymerization of actin filaments [26]. In addition, the elevation of $[Ca^{2+}]_i$ will lead to the activation of Ca^{2+} sensitive K^+ and Cl^- channels and subsequent cell shrinkage which is also known to interfere with cell migration [19].

Acknowledgements

This work was supported by a grant of the Fritz-Bender-Stiftung and Deutsche Forschungsgemeinschaft Schw 407/9-1. The expert technical assistance of Birgit Gassner is gratefully acknowledged.

References

1 Lauffenburger DA, Horwitz AF: Cell migration: a physically integrated molecular process. Cell 1996;9:359-369.
2 Mitchison TJ, Cramer LP: Actin-based cell motility and cell locomotion. Cell 1996;9:371-379.
3 Webb DJ, Parsons JT, Horwitz AF: Adhesion assembly, disassembly and turnover in migrating cells - over and over and over again. Nat Cell Biol 2002;4:E97-100.
4 Aguado-Velasco C, Bretscher MS: Circulation of the plasma membrane in Dictyostelium. Mol Biol Cell 1999;10:4419-4427.
5 Schwab A: Function and spatial distribution of ion channels and transporters in cell migration. Am J Physiol Renal Physiol 2001;280:F739-747.
6 Mandeville JT, Maxfield FR: Effects of buffering intracellular free calcium on neutrophil migration through three-dimensional matrices. J Cell Physiol 1997;171:168-178.
7 Lawson MA, Maxfield FR: Ca^{2+}- and calcineurin-dependent recycling of an integrin to the front of migrating neutrophils. Nature 1995;377:75-79.
8 Eddy RJ, Pierini LM, Matsumura F, Maxfield FR: Ca^{2+}-dependent myosin II activation is required for uropod retraction during neutrophil migration. J Cell Sci 2000;113:1287-1298.
9 Schwab A, Wojnowski L, Gabriel K, Oberleithner H: Oscillating activity of a Ca^{2+}-sensitive K^+ channel. A prerequisite for migration of transformed Madin-Darby canine kidney focus cells. J Clin Invest 1994;93:1631-1636.
10 Carafoli E: Calcium signaling: a tale for all seasons. Proc Natl Acad Sci U S A 2002;99:1115-1122.
11 Lee J, Ishihara A, Oxford G, Johnson B, and Jacobson K: Regulation of cell movement is mediated by stretch-activated calcium channels. Nature 1999;400:382-386.
12 Carafoli E: Calcium-transporting systems of plasma membranes, with special attention to their regulation. Adv Cyclic Nucleotide Prot Phosphor Res 1984;12:543-549.
13 Iwamoto T, Watano T, Shigekawa M: A novel isothiourea derivative selectively inhibits the reverse mode of Na^+/Ca^{2+} exchange in cells expressing NCX1. J Biol Chem 1996;271:22391-22397.
14 Carafoli E: Calcium pump of the plasma membrane. Physiol Rev 1991;71:129-153.
15 Oberleithner H, Westphale H-J, Gaßner B: Alkaline stress transforms Madin-Darby canine kidney cells. Pflügers Arch Eur J Physiol 1991;419:418-420.
16 Dieterich P, Dreval V, Schwab A: Comprehensive analysis of single cell migration. Pflügers Arch Eur J Physiol 2003;445:S44.
17 Grynkiewicz G, Ponie M, Tsien RY: A new generation of Ca^{2+} indicators with greatly improved fluorescence properties. J Biol Chem 1985;260:3440-3450.
18 Schwab A, Finsterwalder F, Kersting U, Danker T, Oberleithner H: Intracellular Ca^{2+} distribution in migrating transformed renal epithelial cells. Pflügers Arch Eur J Physiol 1997;434:70-76.
19 Schwab A, Schuricht B, Seeger P, Reinhardt J, Dartsch PC: Migration of transformed renal epithelial cells is regulated by K^+ channel modulation of actin cytoskeleton and cell volume. Pflügers Arch Eur J Physiol 1999;438:330-337.
20 Kip SN, Strehler EE: Characterization of PMCA isoforms and their contribution to transcellular Ca^{2+} flux in MDCK cells. Am J Physiol Renal Physiol 2003;284:F122-F132.
21 Bordey A, Sontheimer H, Trouslard J: Muscarinic activation of BK channels induces membrane oscillations in glioma cells and leads to inhibition of cell migration. J Membr Biol 2000;176:31-40.
22 Pettit EJ, Hallett MB: Temporal and spatial resolution of Ca^{2+} release and influx in human neutrophils using a novel confocal laser scanning mode. Biochem Biophys Res Commun 1996;229:109-113.
23 Luther PW, Yip RK, Bloch RJ, Ambesi A, Lindenmayer GE, Blaustein MP: Presynaptic localization of sodium/calcium exchangers in neuromuscular preparations. J Neurosci 1992;12:4898-4904.
24 Fujimoto T: Calcium pump of the plasma membrane is localized in caveolae. J Cell Biol 1993;120:1147-1157.
25 Parat MO, Anand-Apte B, Fox PL: Differential caveolin-1 polarization in endothelial cells during migration in two and three dimensions. Mol Biol Cell 2003;14:3156-3168.
26 Downey GP, Chan CK, Trudel S, Grinstein S: Actin assembly in electropermeabilized neutrophils: role of intracellular calcium. J Cell Biol 1990;110:1975-1982.